Shear Stress Induced Thrombogenicity of a Trileaflet Mechanical Heart Valve

Chris Gregan, David Moy, Nicole Newberger, Matthew Siomos

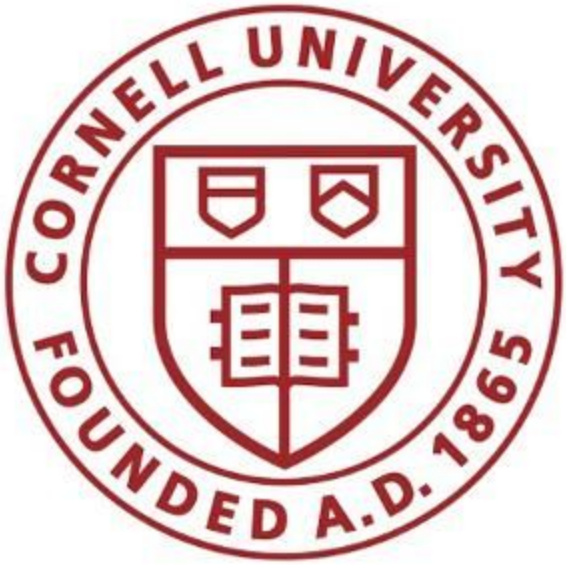

BEE 4530: Computer Aided Engineering - Applications to Biological Processes

Cornell University

Table of Contents

1.0 Executive Summary

Trileaflet mechanical valves are a popular topic in industry R&D due to their potential improvements to hemodynamic performance relative to industry-standard bileaflet mechanical valves and their mechanical durability relative to tissue valves. Novostia is currently attempting to bring their Lapeyre-Triflo trileaflet valve through FDA approvals, demonstrating a clear need and viability for the design concept. While some analysis of this new design has been done, there is a lack of research into the effect of the new leaflet geometry on peak shear stresses in the flow, which impact the thrombogenicity of the valve. Thrombosis is one of the leading causes of complications associated with mechanical heart valves on the market today. While many different factors contribute to the thrombogenicity of a heart valve, high shear stresses in the flow are classically considered to be a significant contributing factor due to the platelet damage that occurs in high shear stress regions.

Specifically, our team examined whether shear stresses and resultant platelet damage are increased relative to classic bileaflet valve designs when the valve is in the open position at peak systole. The triangular leaflet geometry contains a sharp trailing edge, which could increase the shear stresses, and the design also introduces an additional region of flow (four flow regions rather than three), which brings potential for further impacts to shear stress downstream of the leaflets.

2.0 Introduction

The Texas Heart Institute estimates that 106,000 heart valve operations are performed each year in the United States ("Heart Valve…"). A large majority of these surgeries are done to repair or replace the aortic and mitral valves, which pumps oxygenated blood from the lungs through the left atrium, left ventricle and out through the aorta to the rest of the body. Over time, these valves can deteriorate or fail, whether for congenital, biologic, or biomechanical reasons. Since the 1950s, valve replacement surgeries have become an increasingly common solution to the valve failure problem, with a history of constant innovation in device development, always pursuing improved patient outcomes. The history of artificial heart valve development can be gathered into two broad categories; mechanical valves and transcatheter (or biological) valves.

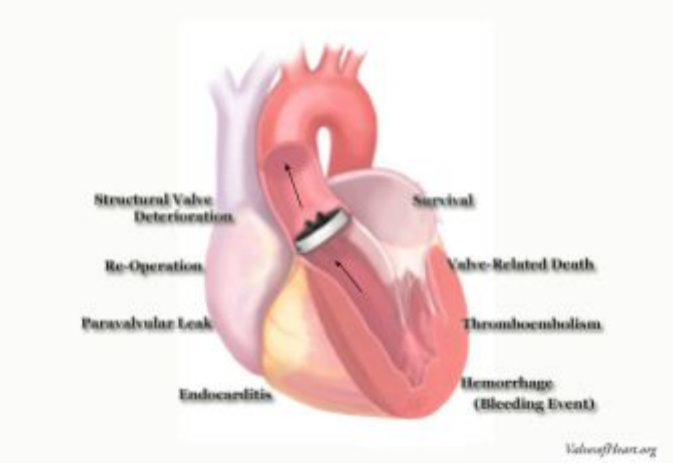

Figure 1: Aortic heart valve position in the body. Blood flows in the direction of the arrows.

Mechanical and biological valve replacements each carry their own strengths and risks. Mechanical valves have long been preferred for younger recipients due to their superior mechanical durability, with mechanical valves typically lasting for the life of the patient without any need for further surgical intervention. However, mechanical valves also introduce biological complications, primarily related to the thrombogenicity associated with the introduction of unnatural materials and non-physiological flow patterns through the valve. The history of mechanical heart valves has included numerous sizeable advancements, both in materials and in more hemodynamically-ideal mechanical designs, but anticoagulation medication is still necessary for all recipients of mechanical heart valves. Biological valves, or tissue valves, solve the thrombogenicity problem of mechanical valves, utilizing natural tissue materials with physiological flow dynamics. However, tissue valve replacements typically experience wear and need to be replaced, often as quickly as ten years after implantation.

There is a strong drive in industry to develop a mechanical valve with improved hemodynamics and reduced thrombogenicity, eliminating the need for anticoagulation medication while maintaining the durability of a mechanical design. Bileaflet valves consist of a circular housing and two hinged occluders that swing open and closed in response to blood flow. They are the current industry standard, as they provide acceptable hemodynamic performance relative to older mechanical valve designs, but bileaflet valve designs fall well short of tissue valves in relation to thrombogenicity and hemolysis that result from blood cell damage. Specifically, some of the primary challenges regarding regarding bileaflet valve performance are:

- Flow cavitation, and resulting turbulence, as a result of the rapid opening and closing dynamics of the bileaflet valve designs. This performance issue is more recently identified as a cause for poor hemodynamics and thrombogenicity in bileaflet mechanical heart valves.
- Hemolysis, or damage to red blood cells, which occurs at shear stresses above 1500-2500 dyne/cm^2 and an exposure time of 102 seconds (Alemu 2007). Hemolysis can occur due to the shear stresses introduced around the bileaflet valve occluders and hinge regions.
- Thrombus formation, which is primarily caused by chronic platelet activation due to shear stress. Thrombi can be generated from shear stresses an order of magnitude lower (100-300 dyne/cm^2) than required for hemolysis (Alemu 2007), making them an even more prominent issue with bileaflet valves, partially driving the need for anticoagulant medication.

Recently, there has been a push to develop a trileaflet mechanical heart valve design, which would provide significantly improved hemodynamics relative to the industry standard bileaflet valves. Novostia, headquartered in Switzerland, is currently in the FDA approval process for their Lapeyre-Triflo valve, which promises no need for anticoagulation therapy traditionally required with all mechanical valves. The Lapeyre-Triflo valve's primary design improvement is associated with improved occluder opening and closing dynamics, which reduces the flow cavitation phenomena that has more recently been identified as a primary driver for poor valve hemodynamics with bileaflet designs. As such, valve opening and closing dynamics has been studied in great detail for the new trileaflet valve design (insert References once we develop our final sources).

However, despite the strong basis of research in trileaflet valve flow cavitation, there has been limited analysis effort towards how the trileaflet design induces shear-stress based effects (hemolysis and thrombus formation), which is a more traditional measure of mechanical valve performance. High shear stresses are introduced in a variety of locations, and at a variety of times throughout the cardiac cycle, but it can be particularly useful to look specifically at shear stresses induced during peak systole. According to a 2012 numerical study, the entire opening and closing cycle of a trileaflet mechanical heart valve is about 320 milliseconds. Of this time, the valve is fully open for 200 milliseconds (Li, 2012). These researchers also noted that the blood reaches its maximum velocity at peak systole when the valve is in the fully open position. The volume of blood passing through the valve in the fully open position is therefore much larger than the amount passing through at any other position. Since both thrombosis and hemolysis are dependent on exposure time and shear stress magnitude, an analysis of the peak shear stresses occurring while the trileaflet valve is fully open is most critical to assessing trileaflet valve performance relative to hemolysis and thrombus formation.

3.0 Problem Statement

The objective of this research is to analyze the fluid dynamics of a trileaflet mechanical aortic heart valve. Specifically this study focused on the peak shear stresses and resultant cell damage occurring while the valve is in the open position under peak systolic flow conditions. These peak shear stresses and damage values compared to values obtained for the classically used bileaflet design.

4.0 Design Objectives (Goals)

This study contributed to the design and optimization of mechanical heart valves in the following ways:

1. Determine fluid flow patterns downstream of the novel trileaflet mechanical valve.
2. Use shear stress to determine resultant cell damage using an experimentally derived damage model.
3. Compare the shear stresses and damage values found to values known for the more commonly used bileaflet valve.

5.0 Geometry and Boundary Conditions

The computational domain is comparable to the geometry as specified by Kadhim, et al. It should be noted that in this research source, the CFD model utilized a bileaflet heart valve. Our schematic, shown in Figure 2, is adapted to include a trileaflet valve as opposed to the bileaflet used by Kadhim, et al. The ventricle before the valve is modeled as a cylinder of diameter 25 mm and length 25.5 mm. The length must be chosen carefully such that the boundary condition specified at the inlet has a negligible effect on the flow behavior of the valve. Figures 4 and 5 present an identical schematic as shown for the trileaflet model. Dimensions of the bileaflet valve is shown in Figure 5. This schematic serves the purpose of validating the implemented damage model which is explained in more detail later in the report.

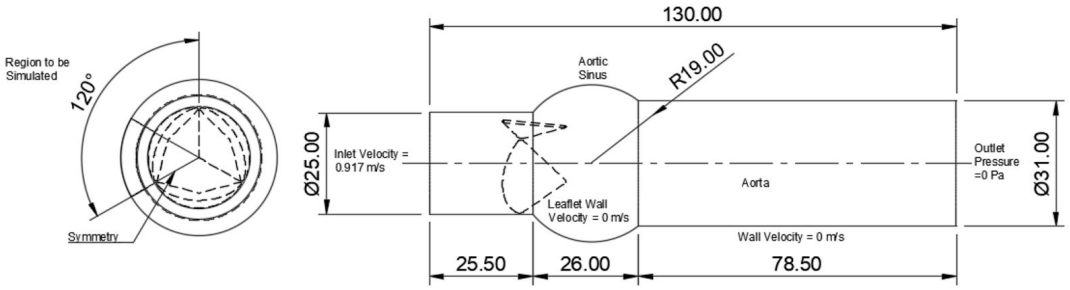

Figure 2. Modelling region of aorta with trileaflet mechanical valve

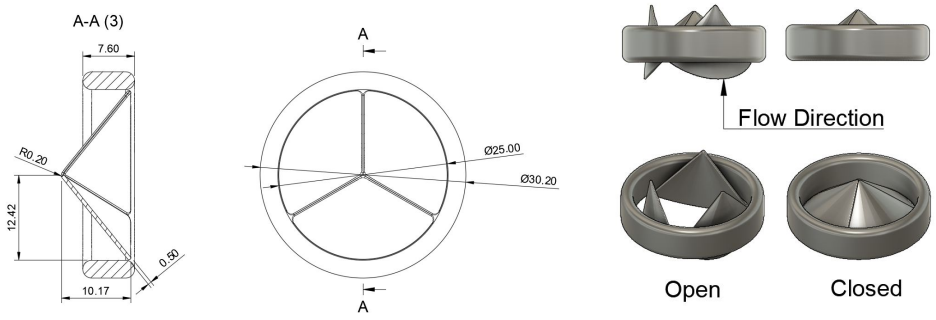

Figure 3. Simplified Tri-leaflet valve CAD Design

The valve leaflets and housing dimensions and parameters are modeled using a similar methodology to that used for the bi-leaflet valve modeled by Kadhim, et al. To simplify the mesh, the hinge mechanism has not been modeled. The trileaflet valve consists of three triangular occluders of a conical shape to minimize the frontal cross sectional area when open. The valves are 0.5 mm thick. The leading and trailing edges have been rounded with a 0.2 mm fillet. Both valves open to a maximum of 85 degrees, pivoting about the lower two corners that contact the housing. The total length of each valve is 12.8 mm.

The aortic sinus is modeled as a sphere, 36 mm in diameter. The sinus blends smoothly from the housing into the aortic valve.

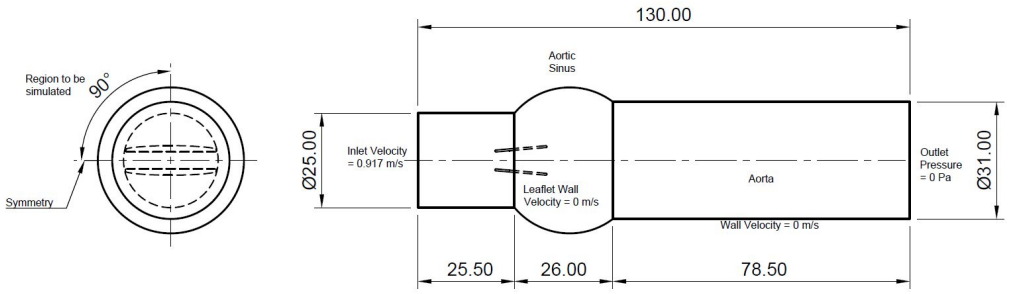

Figure 4. Modelling region of aorta with bileaflet mechanical valve

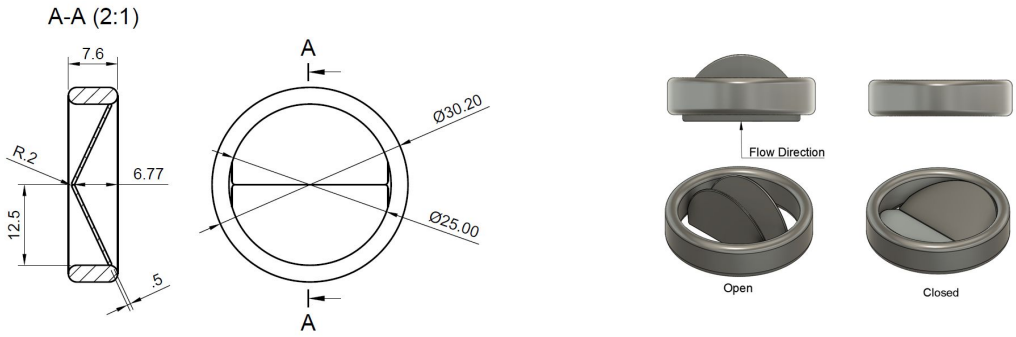

Figure 5. Simplified Bi-leaflet valve CAD Design

The aorta after the sinus is modeled as a cylinder of diameter 31 mm and length 78.5 mm. The length of the aorta must be sufficiently long such that the development of the wake region is allowed to occur naturally and not forced by the end boundary condition. This will affect the flow downstream from the valve. If a curved aortic arch is modeled, as it occurs physiologically, instead of a straight arch, the resulting flow does not display any significant difference at the hinge region, but the arch does result in some asymmetry past the two leaflet valves (Yee Han). However, due to computational limitations, it is not possible to model the entire domain, so we must assume some sort of symmetry. This necessitates the aortic arch be modeled to be straight.

When establishing the boundary conditions for the proposed CFD model of the aorta, there are three main components to consider, as shown in Figures 2 and 4. It is to be noted that all boundary conditions are associated with properties of the flow when the cardiac cycle is at peak systole.

Flow rate at the inlet and pressure at the outlet (downstream of the artificial valve, in the laminar flow region of the aorta) were determined experimentally by Li et. al. 2012. The velocity at the inlet is assumed to be constant and uniform at 0.917 m/s. This value was determined by dividing the flow rate through the aorta at peak systole, 4.5×10^{-4} m^3/s, by the cross sectional area at the inlet, 4.91×10^{-4} m^2. Velocity at

the inlet was modeled as constant, rather than as a fully developed profile for physiological reasons. Blood exits the left ventricle shortly before passing through the aortic valve, therefore fully developed flow is unlikely. The pressure at the outlet was set as a reference and defined as 0. A no-slip boundary condition was assumed for the walls of the aorta and surfaces of the artificial valve.

$v_{in} = 0.917$ m/s
$P_{out} = 0$ kPa
$v_{walls} = 0$ m/s

To reduce computation time, the flow region was split into three 120 degree sections, with zero flow boundary conditions applied at the split faces. However, it has been shown that turbulent flow simulations can be invalid with this assumption if the Reynolds number is over 1,200 (Ge, et al). The validity of symmetry boundary conditions in this model are explored in detail in the appendix.

6.0 Assumptions

Significant model assumptions were made due to computing resource limits and study length limitations. The two major assumptions that differentiate this study from most literature benchmarks are below:

1. Symmetry Boundaries - A 1/3rd circumferential model is utilized, modeling only one leaflet circumferentially
2. Peak-Systole Flow Rate - Flow is only examined during peak systole and the valve leaflets are treated as rigid objects, ignoring the dynamic changes in flow rate and leaflet opening angles throughout the cardiac cycle

6.1 Symmetry:

There is conflicting literature regarding the validity of the symmetry assumption for turbulent flows, like that through a mechanical heart valve. While several computational studies use the 1/3rd symmetry assumption used in this study to reduce computation time, others claim that the turbulent flow characteristics invalidate this assumption. Past studies similar to this one that also use a 1/3rd symmetry assumption include one by Avanzini in 2017, which studied the effect of material properties on the opening and closing dynamics of a trileaflet mechanical heart valve. Additionally, a numerical comparison of bileaflet and trileaflet valves utilized appropriate symmetry conditions in both cases, though it is noted that "the interactions between the geometry and valve orientation will require further investigation" due to other studies' findings that suggest symmetry is invalid(Li et. al 2012).

For instance, a 2007 study by Alemu et. al. states that "the nature of turbulent flow violates imposed geometric symmetry." A study conducted by Ge et. al. in 2003 comes to a similar conclusion for flow through a bileaflet valve. The authors note the development of vortices between the leaflets and the aorta wall. Oscillatory motion of these regions causes a jet-like flow to periodically occur between them. As a result the flow becomes unstable leading to the break of symmetry. However, another study indicates that this may not be the case for trileaflet geometry, and concludes that flow through a trileaflet valve exhibits three-fold symmetry, as shown in Figure 6 (Esquivel et. al.).

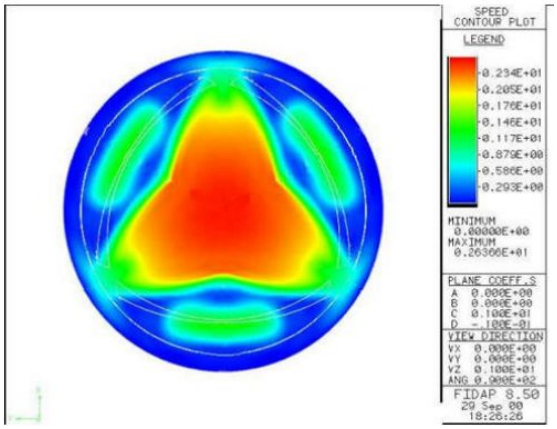

Figure 6: Full trileaflet mechanical heart valve model exhibiting 3-fold symmetry, thereby supporting the symmetry assumption.

Due to this conflicting literature, we decided to run our own simulations of 1/6th, 1/3rd, and full models in COMSOL to see the effect of the symmetry boundary condition in turbulent flows. The results of these studies are shown in the appendix. These studies indicated that the symmetry assumption is not valid given our flow conditions. However, it is possible that the coarse mesh used led to a lack of convergence which have influenced the discrepancies between the three models. However due to computational limitations we were unable to run the full model at a finer mesh. We therefore decided to model a full leaflet with 1/3rd symmetry conditions, as this model yielded results closer to the full model trileaflet then the 1/6th model did and could be run at a finer mesh given our computing resources.

6.2 Peak Systole:

This study examines flow solely during peak systole, or the maximum flow portion of the cardiac cycle, differing from a majority of scientific literature that examines the full cardiac cycle. Examination of flow solely during peak-systole is done to simplify the analysis scope, eliminating the need for inclusion of a second physics in the model to solve for the changing position of the leaflets over time. This significantly reduces computing time, allowing for significantly finer meshes to be solved with the available computing resources and thus allowing for results of interest with much lower, essentially negligible, discretization error.

To validate that flow examination at peak systole provides valid results for shear stresses and resultant shear stress-based platelet activation, one must look first at the theory behind platelet activation and thrombogenicity. Platelet activation results in both chemical and mechanical changes to the cells that increase the likelihood of thrombus formation. When exposed to mechanical forces and stresses over time, platelets activate and secrete procoagulant and self-stimulating substances, while also undergoing a change in shape highlighted by pseudopod extension (Nobili et al, 2008). These changes both serve to increase the strength of adhesion to external surfaces and to reduce resistance to platelet aggregation and thrombus formation (Nobili et al, 2008). It is important to note that platelet aggregation does not occur instantaneously when exposed to a sufficient stress, but instead it occurs over time as a result of damage that builds up due to exposure to various degrees of shear stress. Hellums at al were the first to document

that platelet activation is dependent on the product of shear stress and exposure time (Hellums et al, 1987). However, it has been a challenge to come up with a model of exactly how much shear stress and exposure time is required to activate platelets. Hellums developed an early approximation of the shear stress vs exposure time threshold curve for platelet activation, shown below in Figure 7 (Hellums et al, 1987). They demonstrated that shear stresses on the order of magnitude of 10^4 dynes/cm^2, or 1000 Pascals, would result in platelet damage during the time-scale of peak systole in the cardiac cycle.

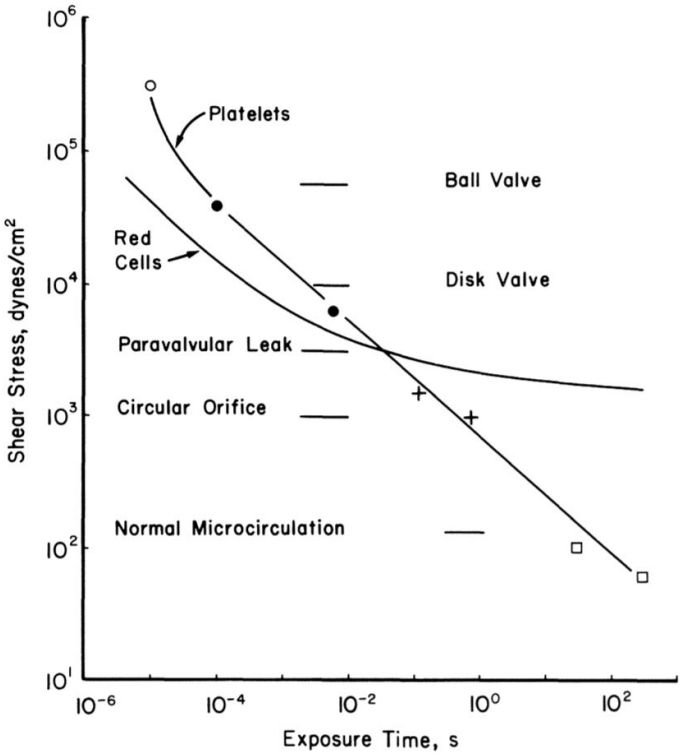

Figure 7: Shear Stress vs Exposure Time Plot showing the threshold of shear stress/exposure time product that results in platelet activation (Hellums et all, 1987)

However, while Hellums is largely regarded as the pioneer of shear-stressed based platelet activation research, his work does not explain why mechanical heart valves tend to damage platelets and increase thrombogenicity, despite inducing lower shear stresses than those of the Hellums criteria. Necessitating further research, a variety of labs have shown that shear stress based platelet damage accumulates over time due to repeated exposure to lower levels of shear stress. Nobili et al ran an experiment exposing platelets to a variety of different shear stress waveforms of low magnitude, 20 dynes/cm^2, which is considered to be the low end of what the bulk flow is exposed to around typical mechanical heart valve prostheses. Their study demonstrated that even at these low levels of shear stress, significant platelet damage occurred after just 30 minutes of cyclic exposure to the 20 dyne/cm^2 shear stress value (Nobili et al, 2008). Nobili et al utilized a chemically modified prothrombinase-based assay to quantify the level of platelet activation, as this assay uses acetylated prothrombin to directly measure the thrombogenic potential and thrombin generation rates. Platelet activation state (PAS), a measure of prothrombinase activity as a fraction of the maximum theoretical activity level, is shown below for a variety of stress

application waveforms. Experimental results are shown by the data points and error bars while theoretically predicted results are shown by the dashed lines.

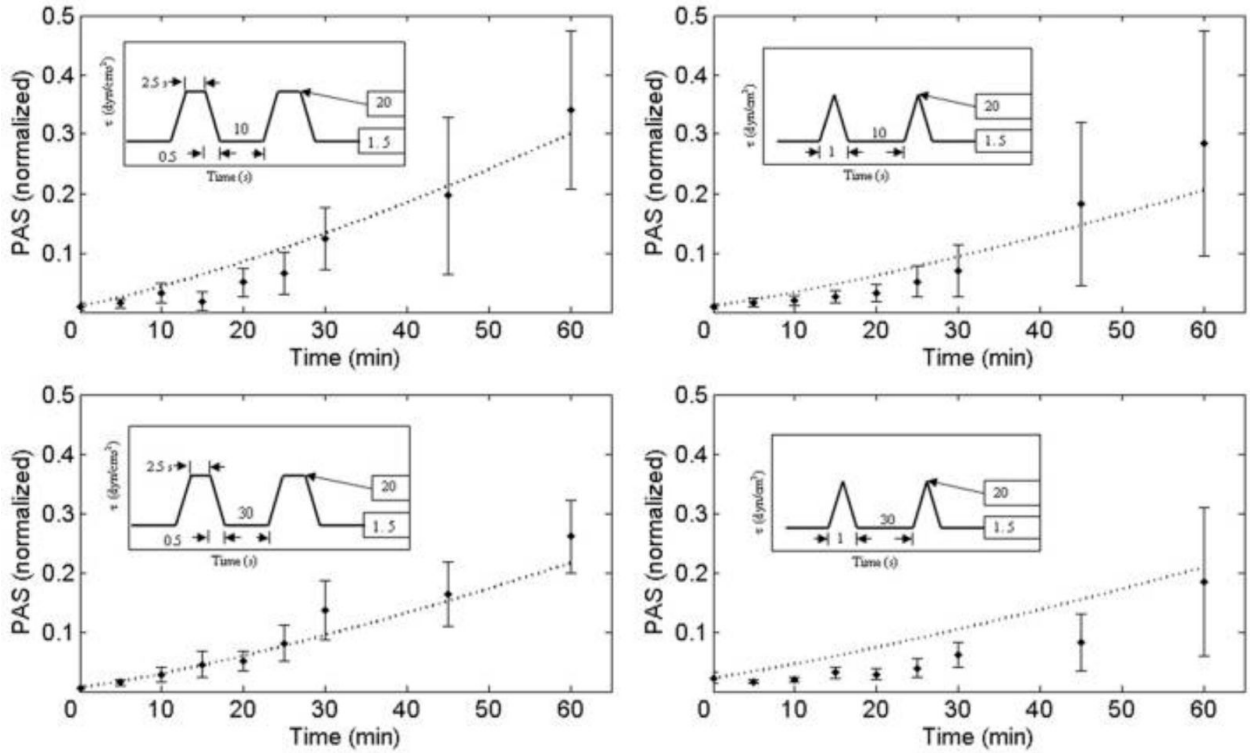

Figure 8: PAS versus time for a variety of applied stress waveforms. Data points and error bars reflect experimentally measured values while the dashed line represents predictions based on a model (Nobili et al, 2008)

Platelet damage accumulation over time at low shear stress values is verified in a variety of other studies as well, such as that of Sherrif et al. Their study looked at a much wider set of stress values and time-based application waveforms, with a matrix of experiments that combined a variety of stress application levels (10-70 dynes/cm^2) with a variety of application waveforms. Ultimately, Sherrif et al's robust set of experiments demonstrates similar PAS levels to those shown in Figure 8 above (Sherrif et al, 2013).

With convincing evidence that time-based exposure to shear stress levels as low as 20 dynes/cm^2, or 2 Pascals, can significantly contribute to thrombogenicity of the valve, it is important also to validate that looking at one flow rate, representing peak systole, is an adequate approximation of the major stress-state seen in vivo. Studies such as Ha et al show that flow rate increases dramatically to peak systole and then returns quickly to 0 and remains roughly constant at 0 for the rest of the cardiac cycle (Ha et al, 2018). Since shear stress is induced by flow rate differentials, and it is typically proportional to increasing flow rates, the low flow rates of the cardiac cycle outside of peak systole are not relevant for studying shear stress-based platelet activation effects. Examining shear stresses during the ramp up to, and down from,

peak systole could yield meaningful results as well, but since the majority of the flow time is spent at peak systole, and shear stress damage is a time-based phenomenon, it is considered valid and conservative to examine flow at peak systole only.

7.0 Governing Equations

Laminar flow is when the fluid flow is steady and smooth. This flow is explained by the Navier-Stokes equations for conservation of momentum. In the initial development of our model we used this assumption.

$$\frac{\delta u_i}{\delta x_i} = 0 \text{ (Incompressibility Continuity) (1)}$$

$$\frac{du_i}{dt} = \frac{\delta p}{\delta x_i} + \frac{1}{Re}\frac{\delta^2 u_i}{\delta x_j \delta x_j} \text{ (Navier-Stokes) (2)}$$

Where u_i are the cartesian velocity components, p is the pressure divided by density (ρ), Re is the Reynolds number, and $\frac{d}{dt}$ is defined as (Sotiropoulos 2009).

$$\frac{d}{dt}(\cdot) = \frac{\delta}{\delta t}(\cdot) + u_j \frac{\delta}{\delta x_j}(\cdot) \quad (3)$$

However, due to the approximate Reynolds numbers in the heart valve, we expect some form of turbulence. Turbulent flow is characterized by unsteady velocity and small eddies that are very computationally expensive to model directly. Reynolds-Averaged Navier-Stokes (RANS) equations model the time averaged behavior of turbulent flow. These reduce the need for computationally expensive meshes, but additional equations are required to model the behavior of the turbulence. We are examining the flow field when it is almost all turbulent, during peak systole when time-dependent shear stress effects are especially relevant, and we are not examining the transition of the flow from laminar to turbulent, so RANS turbulence models are a good approximation. CFD simulations using turbulence models have been validated with artificial heart valve in-vitro experiments (Yee Han).

The k-ω model for turbulence, originally developed by Wilcox (1998), was utilized to model regions of turbulence downstream of the valve leaflets. This model was chosen due to its ability to account for turbulent flow in the transition range, which is commonly present in mechanical heart valves (Alemu 2007). Additionally, COMSOL suggests that the built-in k-ω model can be used for simulations involving internal flows. COMSOL implements the RANS equations and assumptions discussed above through the following equations:

$$\rho(u \cdot \nabla)u = \nabla \cdot [-pI + (\mu + \mu_T)(\nabla u + (\nabla u)^T] + F \quad (4)$$

$$\rho \nabla \cdot (u) = 0 \quad (5)$$

$$\rho(u \cdot \nabla)k = \nabla \cdot [(\mu + \mu_T \sigma_k^*)\nabla k] + P_k - \beta_0^* \rho \omega k \quad (6)$$

$$\rho(u \cdot \nabla)\omega = \nabla \cdot [(\mu + \mu_T \sigma_\omega)\nabla\omega] + \alpha\frac{\omega}{k}P_k - \rho\beta_0\rho\omega^2 \quad (7)$$

$$\mu_T = \rho\frac{k}{\omega} \quad (8)$$

$$P_k = \mu_T[\nabla u : (\nabla u + (\nabla u)^T)] \quad (9)$$

Shear rate was used to compute the shear stress within the model. The shear rate is an inbuilt COMSOL function that computes the rate at which fluid layers move past each other. The shear stress is defined as the shear rate multiplied by the viscosity.

$$\tau = \mu * \Sigma[\frac{\partial v_i}{\partial x_j} + \frac{\partial v_j}{\partial x_i}] \quad (10)$$

8.0 Model Setup

The team started with a k-ω turbulence model, utilizing the input parameters and boundary conditions indicated previously. The turbulence model was run with default k-ω parameters.

Meshing was completed in sections, with one volume region and three surface regions. The volume region included the entire fluid body. The first surface region is composed of the outer walls of the aorta. The second region includes the walls of the valve and leaflet. The third region includes the leading and trailing edges of the leaflet. These sections were chosen after preliminary runs of the model with a very coarse mesh showed which regions were most important for convergence. The meshes were adjusted by varying the COMSOL preset (coarse, fine, etc) defined meshes in each individual region.

The convergence criteria was chosen as the average shear stress on the leaflet edges. This is because it is the primary subject of this study, as the parameter that directly influences heart valve thrombogenicity. Additionally, shear stress was shown to be highest on the leaflet edges. The mesh settings and the maximum shear stress are summarized in Table 1.

The fluid properties that were utilized were those representing the properties of whole blood, approximated as a Newtonian fluid. Density was set to 1070 kg/m^3 and viscosity was defined as 0.0039 Pa s.

Table 1: Mesh Convergence Data

Mesh Settings									Mesh Data	
	Max Element Size				Min Element Size					
Mesh Number	Volume	Outer Wall	Valve Faces	Valve Edges	Volume	Outer Wall	Valve Faces	Valve Edges	Domain Elements	Average shear stress on the leaflet edges (Pa)

1	2.47	1.66	1.31	1.31	0.714	0.494	0.247	0.247	317950	45.424
2	1.66	1.66	1.31	0.914	0.494	0.494	0.247	0.0988	1381219	58.085
3	1.66	1.31	0.914	0.568	0.494	0.247	0.0988	0.0371	2975125	61.06

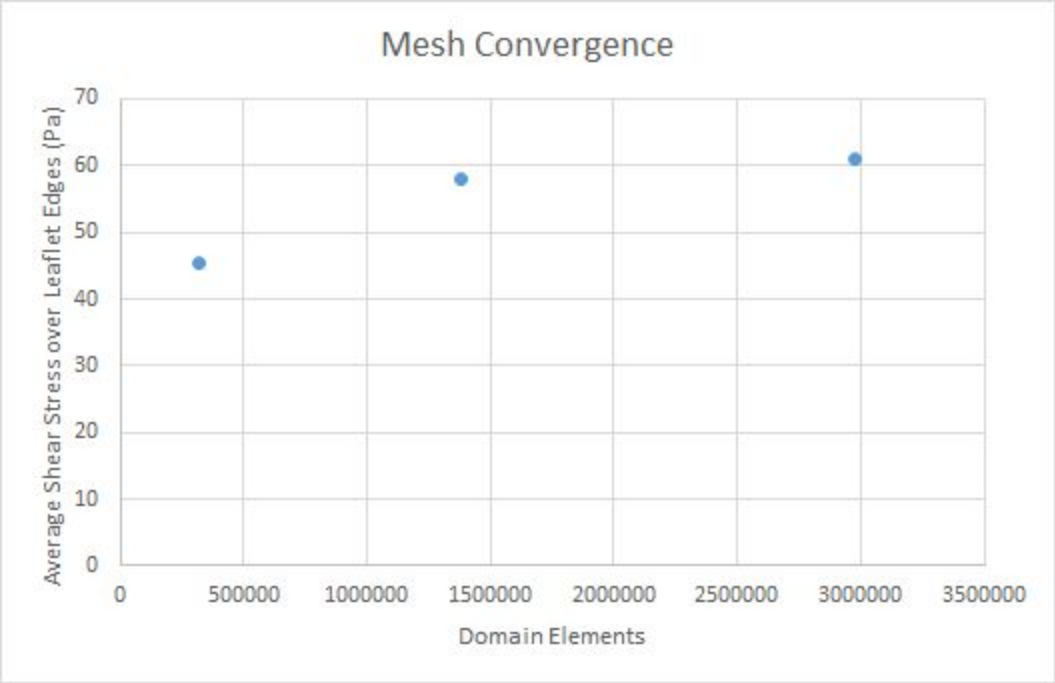

Figure 9: Average shear stress on the valve leaflet edges converges with successively refined meshes.

The average shear stress over the leaflet appears to converge to within 5% difference at Mesh 2. This mesh was therefore used for analysis.

8.1 Damage Model

While the effect of shear stress on blood cells is complex, it is possible to represent general cell damage as a function of shear stress. The damage model that was developed provides information about the cumulative damage that platelets experience due to shear stress exposure. Therefore this model is accounting for damage the platelets may have experienced on previous passes through the mechanical heart valve, assuming the cells have "perfect" memory. The damage rate model is represented below, which was formulated by Yeleswarapu et al.

$$\dot{D}(t) = \left(\frac{\sigma(t)}{\sigma_0}\right)^r \frac{1}{[1-D(t)]^k} \qquad (11)$$

The constants σ_0, r, and k are determined by experimental data. The damage rate model provides insight of damage growth to the platelets which was categorized into three stages. Integrating the equation, an expression for the damage accumulation can be obtained as shown.

$$D(t) = D_0 + \frac{1}{\sigma_0^r} \int_{t_0}^{t} \frac{\sigma(\tau)^r}{[1-D(\tau)]^k} d\tau \quad (12)$$

Where $\sigma(\tau)$ and $D(\tau)$ are the shear stress and damage histories, respectively, and D_0 is the initial damage at time $t = t_0$. This model provides a normalized value output ranging from 0 to 1. In this application, zero represents no activation and 1 represents full activation.

This theoretical model operates under a series of assumptions. It was assumed that the platelets will follow the same flow trajectory during each passage through the heart valve, conservatively approximating the time taken to activate a platelet. The worst case flow trajectories are examined, consistent with the literature. Additionally, as mentioned within the damage rate model, it was assumed that the platelets withheld a "perfect memory" and no damage is recovered after returning on the next path through the valve.

The damage model was implemented using a massless particle tracking study. As such, there are no physical parameters for the particles that are needed. The particle tracking study calculates the path of the blood as it flows through the valve using the velocity field from the fluid dynamics study according to the following governing equation:

$$\frac{dq}{dt} = v \quad (13)$$

Where q is the path of the particle and v is the velocity of the fluid. The particle path will follow the direction of the velocity as it travels through the leaflet. The particles are simulated over a period of 0.8 seconds.

The damage was calculated by defining the damage rate in accordance with the equation shown above and numerically integrating it over the path of each streamline. 20,000 particles were released with a random distribution on the inlet surface. This number was determined by a convergence analysis on the average damage of the particles (see appendix).

9.0 Results and Discussion

As a visual check, the flow velocity around the valve was examined. The flow was examined through two radial planes; one through the center of the leaflet to capture the maximum downstream effects from the leaflet, and another along the edge of the model in the region where the leaflet hinge occurs. The fluid velocity plots show a large velocity increase through the central orifice in the plane central to the leaflet, which is approximately what is expected.

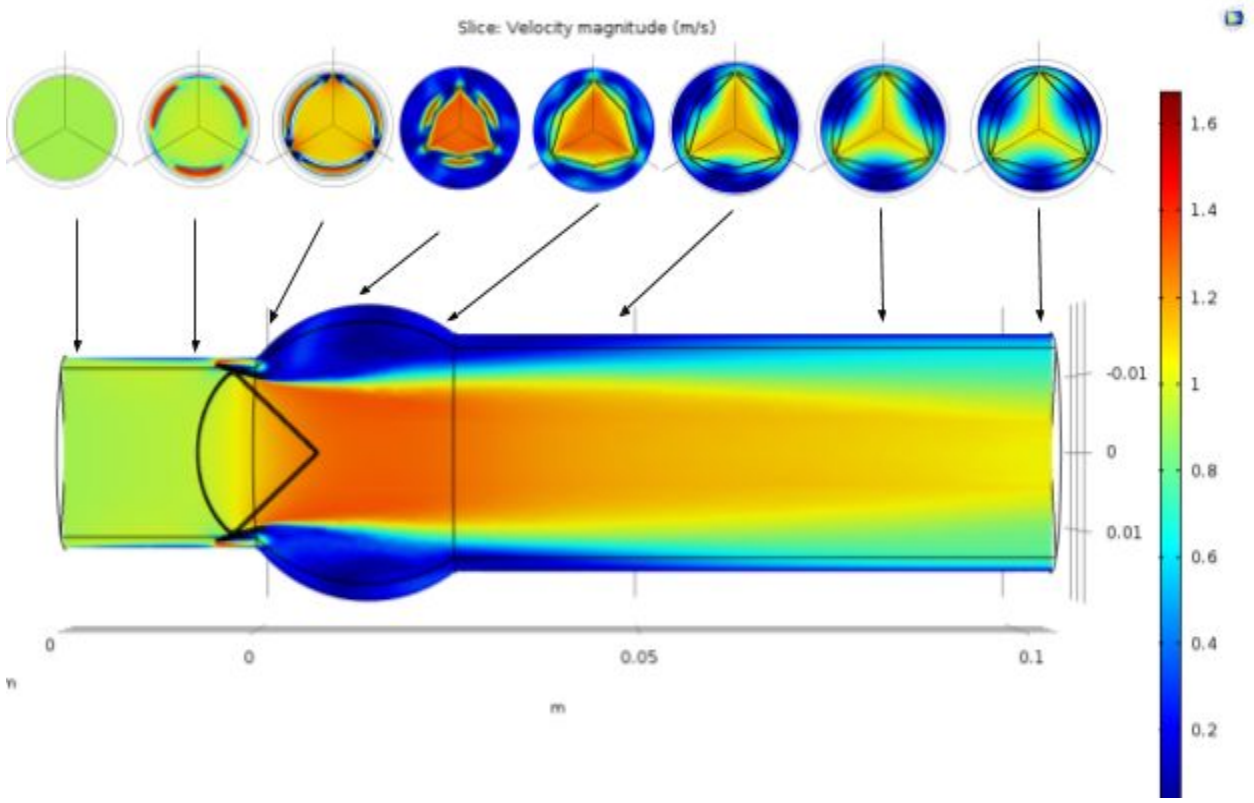

Figure 10: 2D velocity plot showing flow velocities through the center of the leaflet (top) and in the radial plane near the edge of our model, at the corner of the leaflet (bottom). X-Z plane cross sections are included at different points along the flow (legend on the right refers to these cross sections). Results from the mesh 3 study are shown.

As stated before, the maximum shear stress around the valve occurs at the leading edge of the valve. There also appears to be a region downstream from the trailing edge that produces elevated shear stresses. The shear stress magnitude appears to decrease as the flow continues downstream. The peak shear stress region is very concentrated to the entire leading edge. This is the reason for the high amount of damage on the flow trajectories over the top of the valve.

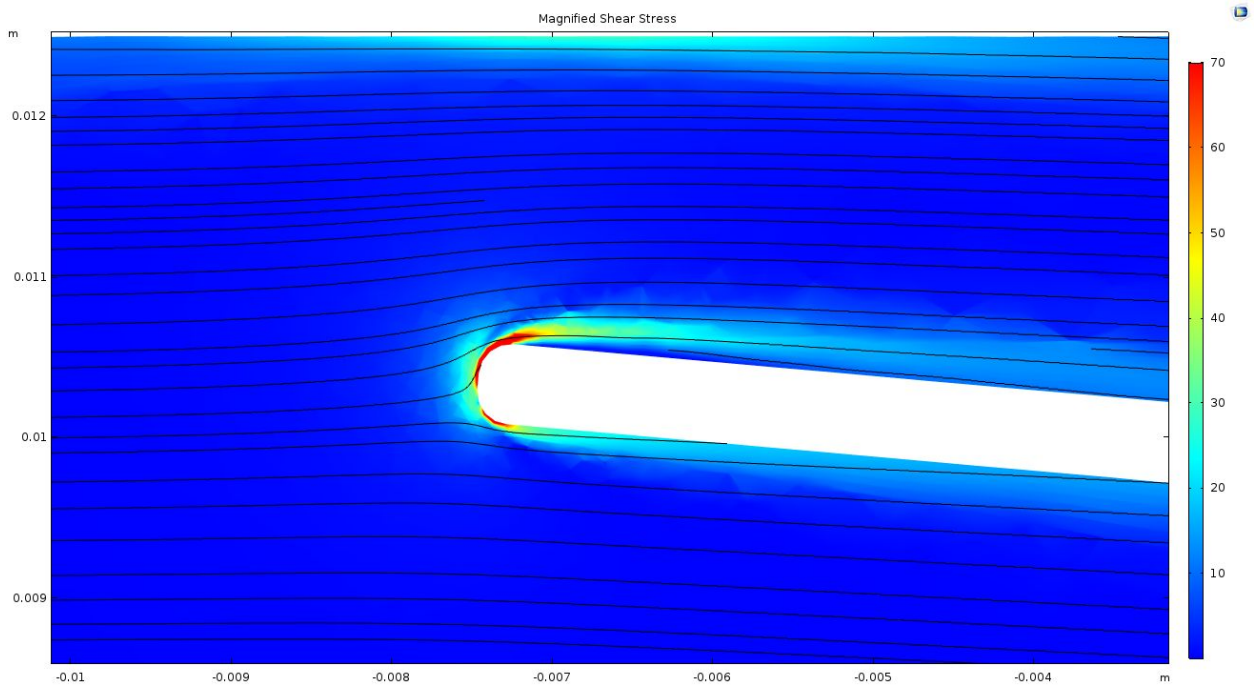

Figure 11: Magnification of the shear stresses around the wall of the valve in the radial plane through the center of the leaflet. Note the color scale has been magnified to show the shear stress differences in regions of low shear. Only a small percentage of the fluid streamlines pass through the region of high shear stress.

While the trileaflet design provides improved performance in many aspects, this increase in peak shear stress is notable due to the shear stress' potential effect on valvular thrombogenicity.

9.1 Damage Model Implementation

The resulting streamlines and damage of the blood flow in the valve shows an interesting result. The particles with damage below 1E-5 have been hidden, showing that the platelets that hit the leading edge of the leaflet are at the most risk of activation, as shown by Figure 12.

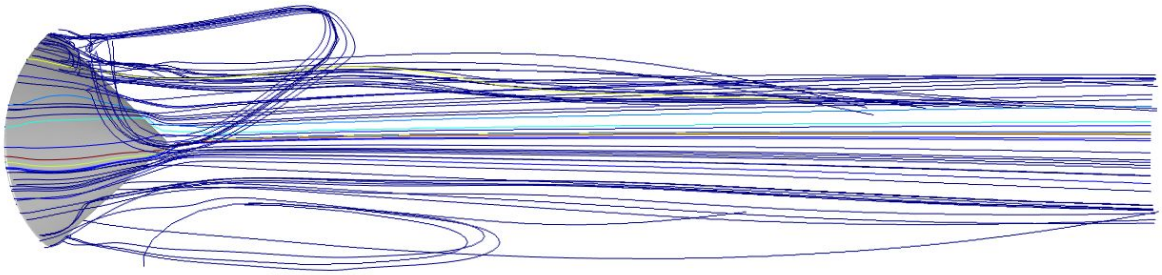

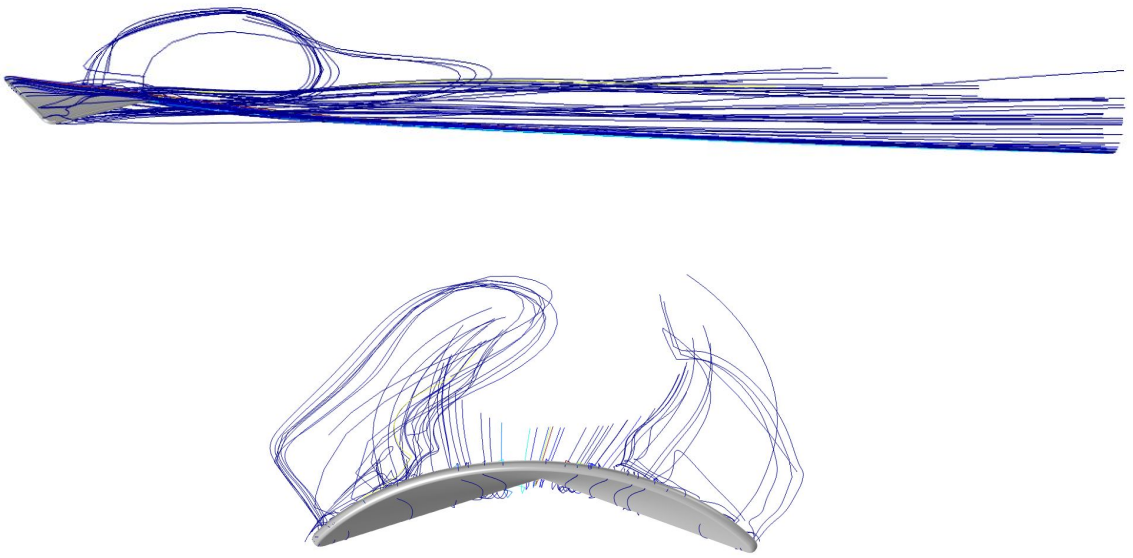

Figure 12: Only the high damage particles over the leaflet are shown. Blood hits the leading edge of the leaflet and accumulates damage. Some blood continues down the artery while blood near the hinges recirculates in the sinus.

The maximum damage a fluid particle experiences as it exits the outlet is 0.01872. The average damage of all the particles is 1.021×10^{-5} with a standard deviation of 3.094×10^{-4}. This is because the damage simulated by the particle tracking is very sensitive to the distance between the fluid path and the leading edge, as shown by figure 9. Paths very close to the valve edge travel through a region of high shear stress and travel along the valve face, and consequently accumulate much more damage.

There also appears to be a low velocity recirculation region in the aortic sinus. The particles spend a long amount of time in the sinus, so the particles seem to accumulate damage even though the shear stress is low.

Figure 13 shows the average damage of all of the simulated particles. There is a sharp spike in damage after 0.020 seconds as the particles hit the leading edge of the valve. There is then a slow accumulation of damage as the particles travel in the leaflet boundary layer until 0.08 seconds.. After the particles clear the leaflet, there is a negligible amount of damage.

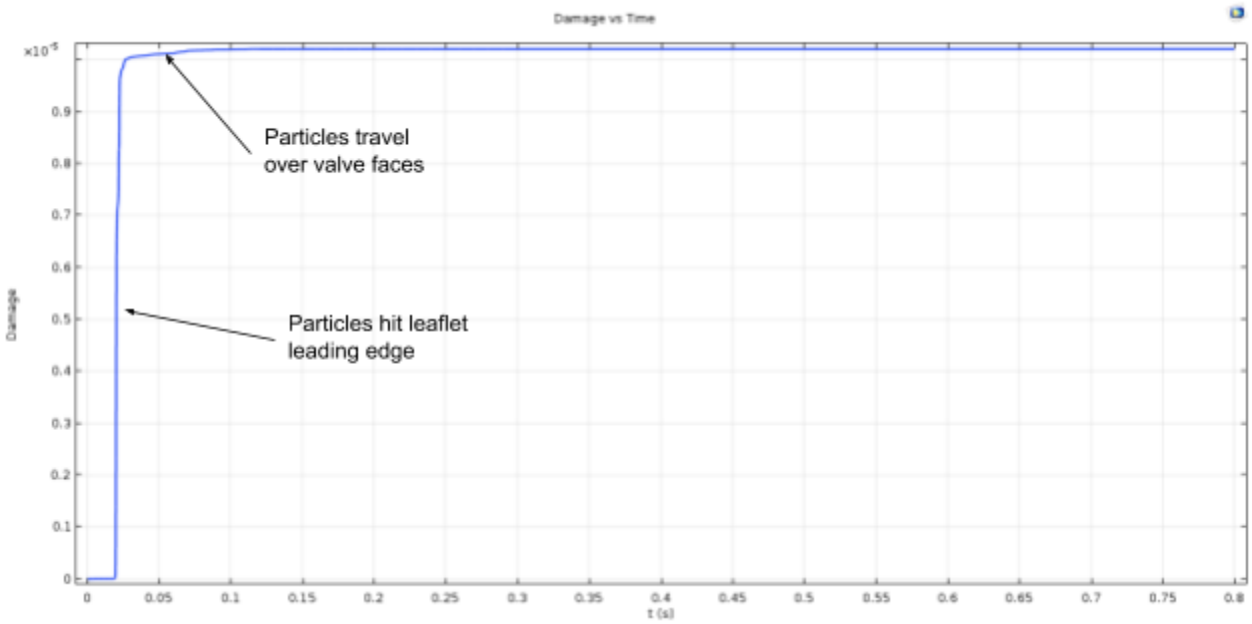

Figure 13: Average damage of the particles over time.

A histogram of the damage shows the distribution of the damage across the particles. It shows that the vast majority of particles accumulate little to no damage.

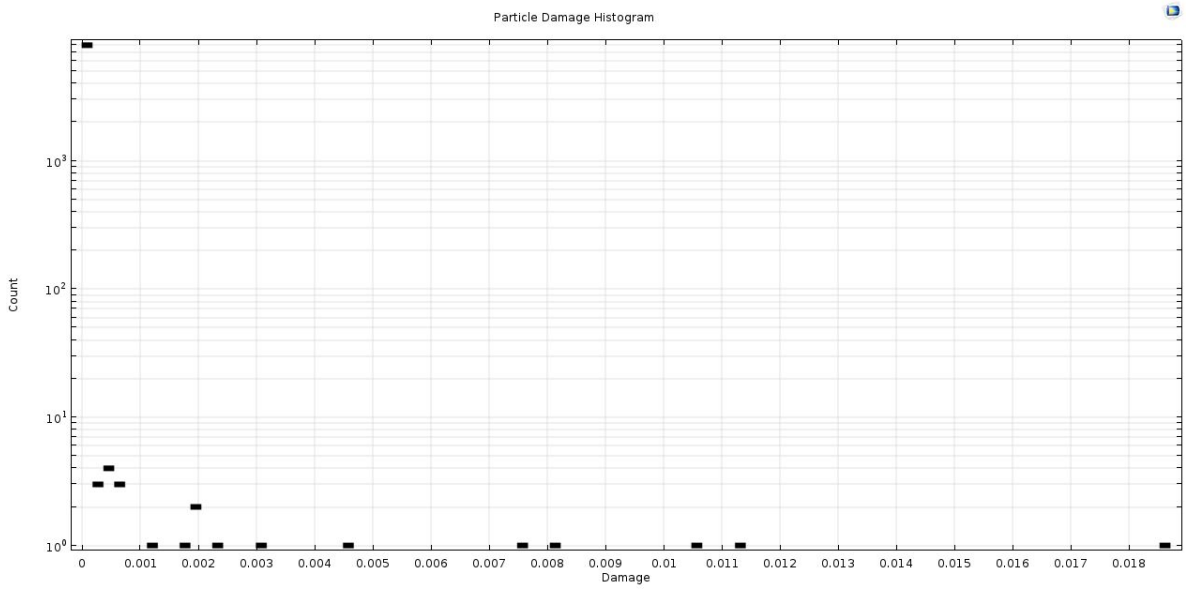

Figure 14: Shear stress histogram. This suggests that only a small fraction of blood is damaged as it travels through the valve.

9.2 Comparison With the Bileaflet Valve

The bileaflet valve model velocity plot is shown below. It shows the three distinct high velocity jets the blood takes as it flows through the valve. The jets gradually merge to be more uniform downstream. The upper and lower jets expand outwards towards the wall.

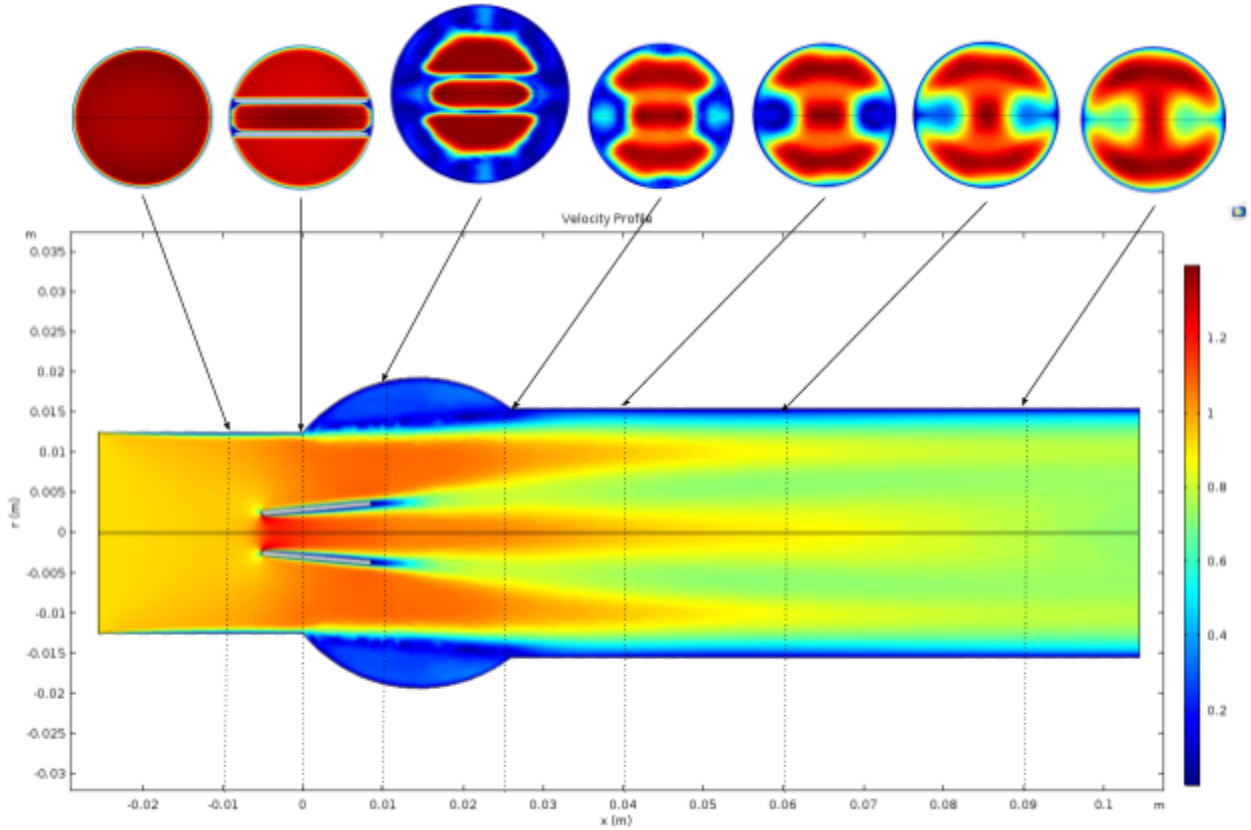

Figure 15: 2D velocity plot showing flow velocities through a cross section of the artery (top) and in the plane of symmetry(bottom). X-Z plane cross sections are included at different points along the flow.

The damage model is run on the the bileaflet valve. Again, only the high damage particles from the leaflet are shown.

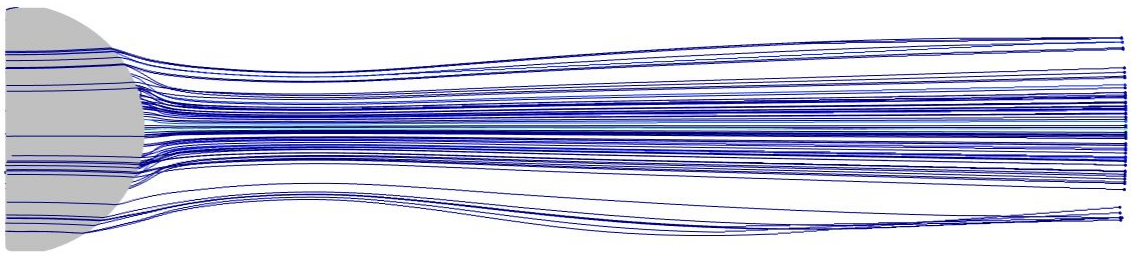

Figure 16: Bileaflet High Damage particle flow paths. The majority of the damage occurs as the fluid hits the leading edge of the valve.

Once again, The damage occurs as the high velocity flow hits the leading edge of the leaflet.

Table 2 compares the average and maximum damage of the particles in the trileaflet valve to the bileaflet valve. The trileaflet model's damage was found by averaging the results from the 8000, 12000, 16000, and 20000 particle simulations.

Table 2: Damage Comparison between the Bileaflet and Trileaflet valves

Model	Maximum Damage	Average Damage
Bileaflet	0.015	3.06×10^{-6}
Trileaflet	0.034	9.57×10^{-6}

The results suggest that the flow characteristics of a trileaflet valve at peak systole is more thrombogenic than a bileaflet valve.

Based on the plot of damage over time, it can be deduced that the majority of damage occurs on flow over the leading edge of the valve. Therefore, it is necessary to compare the flow and shear stress over the two different valve leaflets.

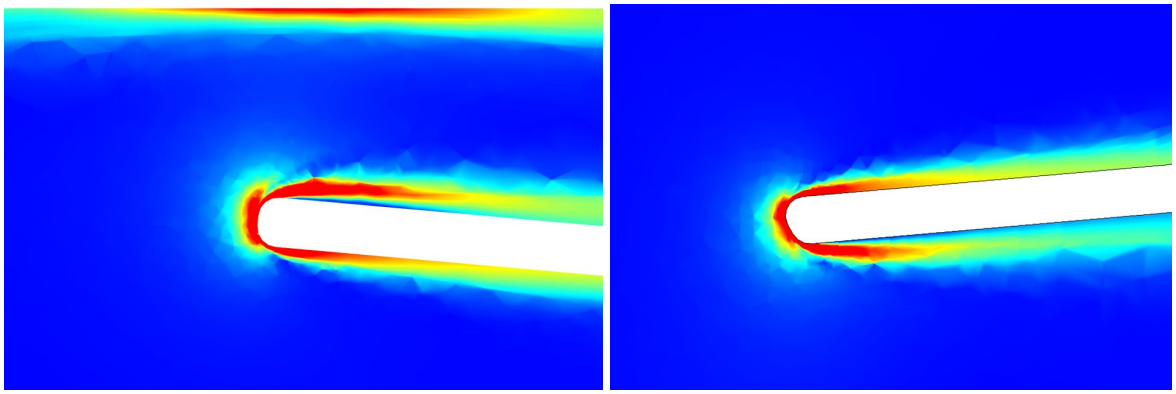

Figure 17: Shear Stress over the leading edge of the trileaflet (left) and bileaflet (right) valve leading edges. The maximum shear stress in the trileaflet valve is 245 Pa and the maximum in the bileaflet valve is 218 Pa. The average shear stress over all of the leaflet edges (leading and trailing) of the trileaflet valve is 58.0 Pa. The bileaflet is 43.8 Pa. There is also higher shear stress along the wall close to the leading edge of the valve.

Table 3 shows the shear stress maximum and averages across the leading and trailing edges of the valves. The bileaflet valve has lower shear stress. Therefore, it makes sense that there is less damage in the flow that hits the leading edge.

Table 3: Shear Stress values over the leading and trailing edges of the valve.

Model	Average Edge Shear Stress	Maximum Edge Shear Stress
Bileaflet	43.8	218
Trileaflet	58.0	245

Shear stress is proportional to the shear rate, which is proportional to the velocity gradient of the fluid. Therefore, the higher the velocity increases as it travels through the valve, the higher the shear stress. The normalized velocity profiles of the bileaflet and trileaflet valves are shown in figure 18.

This is likely due to the very narrow flow region between the exterior wall of the aorta and the leaflet in the trileaflet valve model, which generates a very high velocity gradient around the leaflet leading edge and through this region. Bileaflet valve designs separate the flow into three regions, with the two exterior regions being much wider (with resulting much more gradual velocity gradients) in comparison to the exterior region in the trileaflet valve. This is shown in figure 18, which plots the velocity of the flow through the center of the valve.

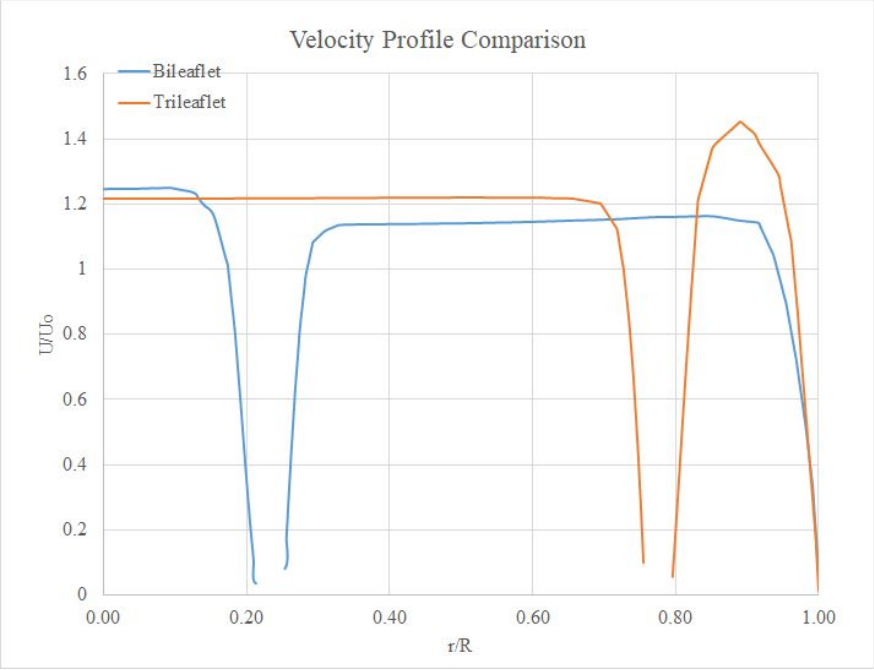

Figure 18: Velocity profiles at the center of the valve over one leaflet.

10.0 Validation

Validation of the results of this study is threefold. First, the flow velocity downstream of the trileaflet valve was compared to data found in several studies. Secondly, we sought to validate the shear stresses computed by the model. There is a lack of literature pertaining to shear stress in trileaflet valve flow simulations. There is however a good amount of data on shear stress in bileaflet models. Since shear stress is an important parameter in this study, a bileaflet model was also constructed in COMSOL with equivalent setup to the trileaflet valve except for the valve geometry itself. This bileaflet model was then used to validate against literature, with the assumption that this validation carries over to our near equivalent trileaflet model. Any discrepancies between the two can be attributed to geometrical impact, as all other factors are held constant. Finally, damage model results between our bileaflet and trileaflet model were compared, and validated against another study which made use of the same model, though they implemented it in a slightly different way.

10.1 Flow Velocity in Trileaflet Model

To validate the velocity downstream of the heart valve, velocity parameters found in literature for other mechanical trileaflet heart valve CFD simulations were utilized for comparison. Velocity was validated in two different approaches, with maximum velocity, and observing the velocity profile one diameter length downstream from the heart valve. These parameters were compared for models found in literature that were most similar to our model in COMSOL, hence, ensuring a level of accuracy when comparing the two. Firstly, the maximum velocity through the orifice of the heart valve was analyzed. Based upon the design of a heart valve, at peak systole, a velocity jet will result at the centre orifice of a valve. Peak velocity provided from Li and Lu was seen to be 1.55 m/s, which was compared to our peak velocity of 1.67 m/s. While their model provides one of the best comparisons from literature, there were slight variances that could account for this variation in maximum velocity. For instance, their effective orifice area was not of equivalent size, which would heavily dictate the maximum velocity. Secondly, the flow rate that was obtained at peak systole was smaller, contributing to a difference of maximum velocity.

To further validate the velocity flow of the model of this study, the velocity profile downstream was observed. This comparison validation utilized CFD simulations conducted by Yee Han. The Yee Han model, including the aortic arch, but in comparing velocity profile results 1 diameter length downstream of the valve, arch effects are considered to be minimal. Figure 19 shows where the 1 diameter downstream cross section is located, significantly prior to where the arch effects dominate.

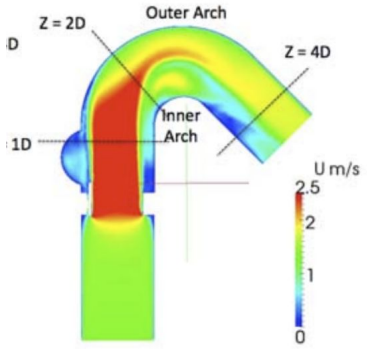

Figure 19: Schematic of Yee Han Model. Location of Velocity Plane Comparison (1 diameter length from valve)

To normalize the comparison, a velocity profile for our model was analyzed at 1 diameter length away from the valve. Figure 20 shows the comparison of the velocity profile at 1 diameter length away from the valve in each respective model (The green line graph represents the tri leaflet valve). The velocity profiles did not match qualitatively, however the overall shape of the profile from our model did replicate a similar profile to that found from Yee Han. The variation in velocity values could be due to the difference of diameter for the heart valve, the inclusion of the aortic arch, and different inlet and outlet boundary conditions.. Overall, this validation offers positive signs that the model is replicating velocity profiles similar to literature.

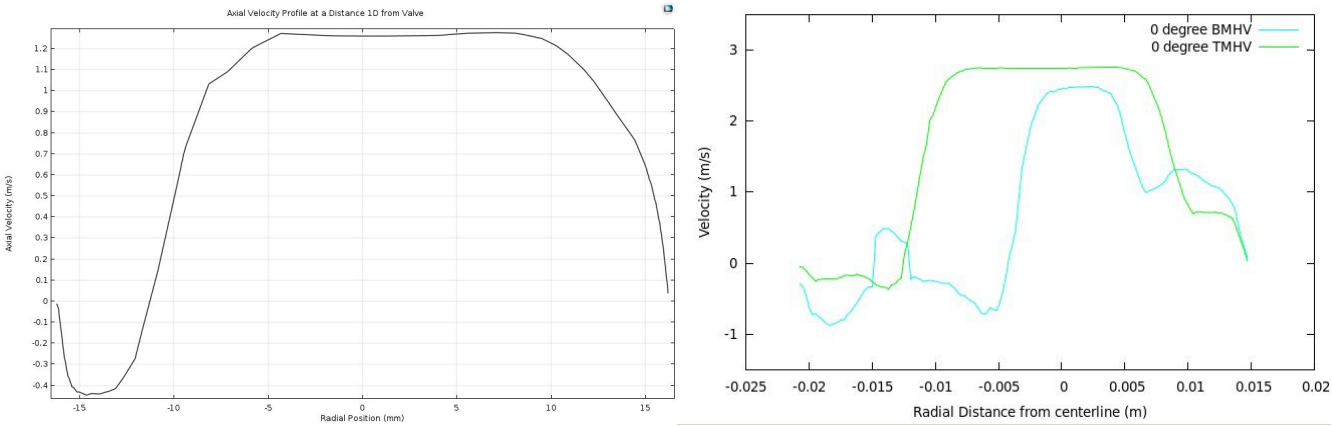

Figure 20: Velocity profile comparison at 1 diameter length away from heart valve location. Left: our comsol model. Right: Model presented by Yee Han.

10.2 Shear Stress in Bileaflet Model

There is a lack of experimental shear stress measurements in literature. In order to help validate our model, the shear stress computed by the bileaflet model will be compared to experimental data measured by Woo, Yoganathan (1986). The experiments were conducted using laser doppler anemometry and

analyzed the full pulsatile cycle. The fluid was a blood analog with a density of 1050 kg/m^3 and a viscosity of 0.0035 Pa s.

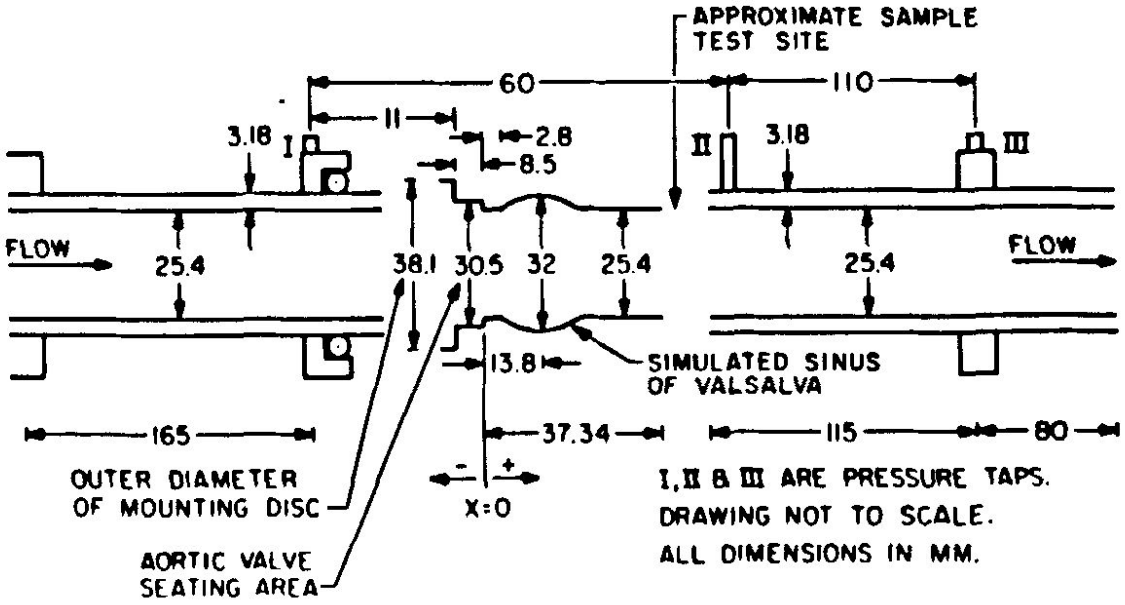

Figure 21: Experimental apparatus used by Woo, et al (1986).

The experimental measurements were taken at various cross sections downstream from the valve. The measurements are compared to the computed values below.

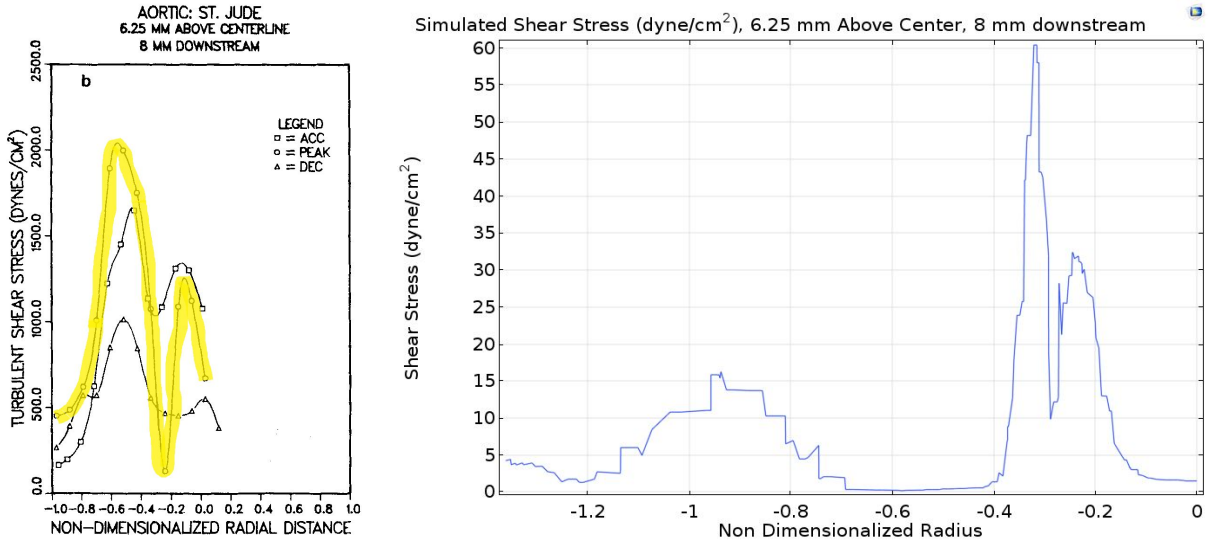

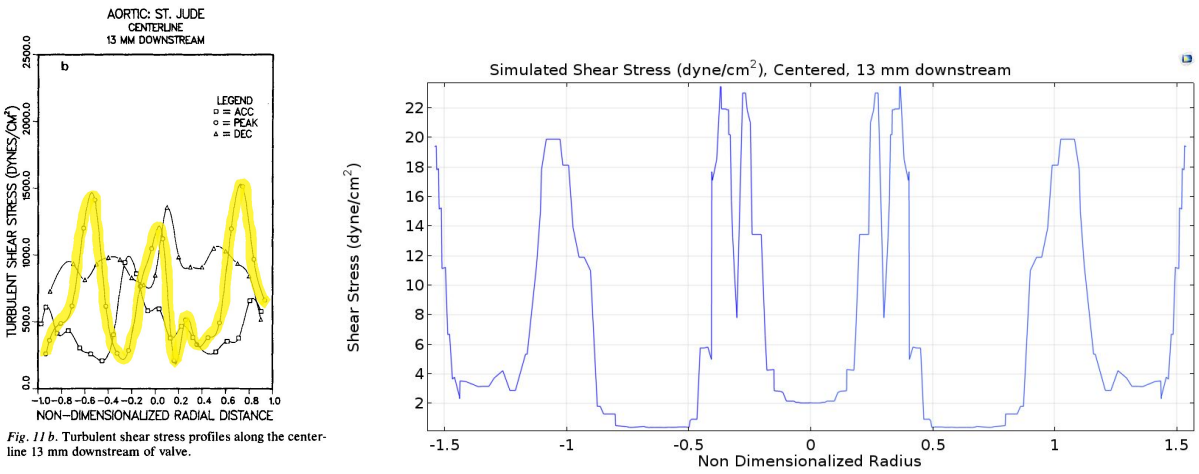

Figure 22: Shear stress profiles from experimental data (left) and simulation (right). The upper data was taken from 8.25 mm downstream and 6.25 mm offset from the center of the valve.. The lower data was taken 13 mm downstream and at the center of the valve.

The comparison to experimental data qualitatively matches the simulation. However, the magnitude predicted by our simulation is much lower than anticipated. One possible explanation could be the difference in flow velocities used to test. The velocity 8 mm downstream of the valve in the experiment is 2.25 m/s, while the simulated velocity is only 1.1 m/s. Sensitivity analysis shows that the increase in shear stress is non-linear with velocity, so a small increase in velocity could result in a large increase in shear stress. The team acknowledges that the numerical values are likely erroneous, but believes the qualitative comparison of the data is accurate enough that the group can compare the two valves accurately.

Other simulations predict similar numbers as the team's model. Dasi et al, record a 150 Pa peak shear stress for CFD analyses of bileaflet mechanical heart valves. The team's simulation predicts a maximum of 218 Pa over the leading edge, which is in the same order of magnitude.

11.0 Sensitivity Analysis

Sensitivity analysis was performed on our model to provide insight into understanding how platelet activation would be affected by variations in certain physiological parameters. The parameters chosen for the sensitivity analysis were based upon physiological parameters that are likely to change for the patient demographic that would be susceptible to having a heart valve replaced.

11.1 Velocity Input

The input velocity was varied to reflect different flow rates at peak systole. This is especially important because different peak systole flow rates can be found in different literature sources and different subjects. By evaluating the effect of flow rate on peak shear stress, we can identify the importance of flow rate on thrombogenicity of the valve. Flow velocity at the inlet will be varied between 0.2 m/s and 1.43 m/s, in accordance with minimum and maximum in vivo measurements of flow velocities (Garcia et al, 2017). Based upon the sensitivity analysis completed with the mentioned velocity values, it was shown

that the damage possessed an exponential increase trend as shown in Figure 23. For velocity values below 1m/s, the damage of the platelets stayed between a range of 0 - 0.06, however beyond this velocity a rapid increase in damage was seen. Completing future sensitivity analysis beyond the 1 m/s threshold would be advisable in providing a better representation of the exponential relationship of platelet damage and inlet velocity to the model.

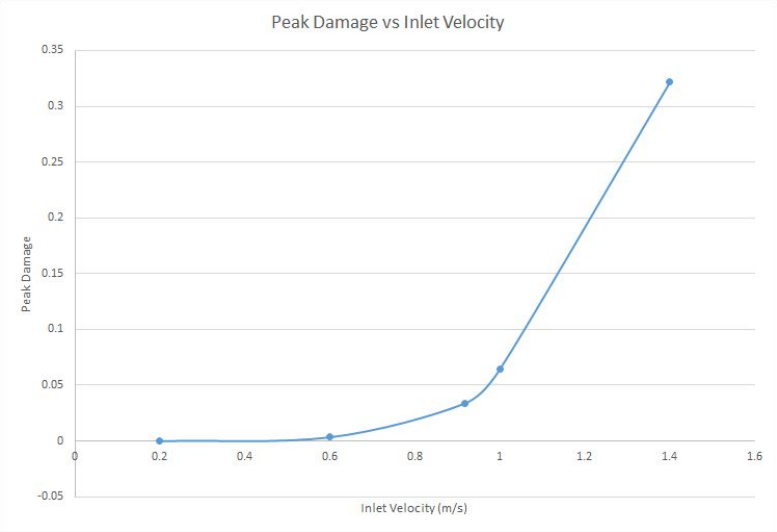

Figure 23: Variation of velocity inputs (0.2 m/s - 1.43 m/s) with the corresponding peak damage occurrence for platelets

11.2 Viscosity

The varying of viscosity for whole blood was completed to account for different individuals who possess different blood viscosities as a result from medical conditions explained in literature. Since this was the reasoning of completing the sensitivity analysis, minimal data on patients experiencing a large range of viscosity values, and was only seen that patients are typical to experience viscosity values higher than average. For patients receiving a mechanical heart valve transplant, it is probable they will be at larger risk for certain cardiovascular diseases. Therefore, a simulation was completed for the trileaflet model for a whole blood viscosity of 0.0052 Pa-s which was verified by Celik et al, that this is the value to which patients will experience a lower survival rate due to cardiovascular diseases. It was seen that damage of the platelets was not largely sensitive to the variation of the viscosity. There was a proportional increase of platelet damage from the increase of viscosity from 0.0039 to 0.0052 Pa-s, however no unusual results were drawn from this analysis. To conclude the increase of damage was to be expected based upon these patients experiencing a larger increase of cardiovascular diseases which can be resultant from thrombogenicity.

12.0 Design Consideration of Valve

It has been identified that platelet damage comes primarily from the flow sections around the leading edge of the leaflets and over the leaflet surface. Acknowledging this, it is clear that significant design effort

should be placed into these items, with FEM analysis serving as a potentially critical part of the design process, as described below.

12.1 Leaflet Leading Edge Optimization

The first design recommendation flowing from our analysis is in regards to the leaflet leading edge radius, a critical area for shear stress and platelet damage. A leaflet with rounded edges will deflect the flow around it more gradually, lowering the velocity gradient and shear stress. This can be demonstrated with a 2D axisymmetric model under the same conditions as a 3D model. The leading edge radius was varied from 0.1 mm to 0.25 mm (a smooth curvature).

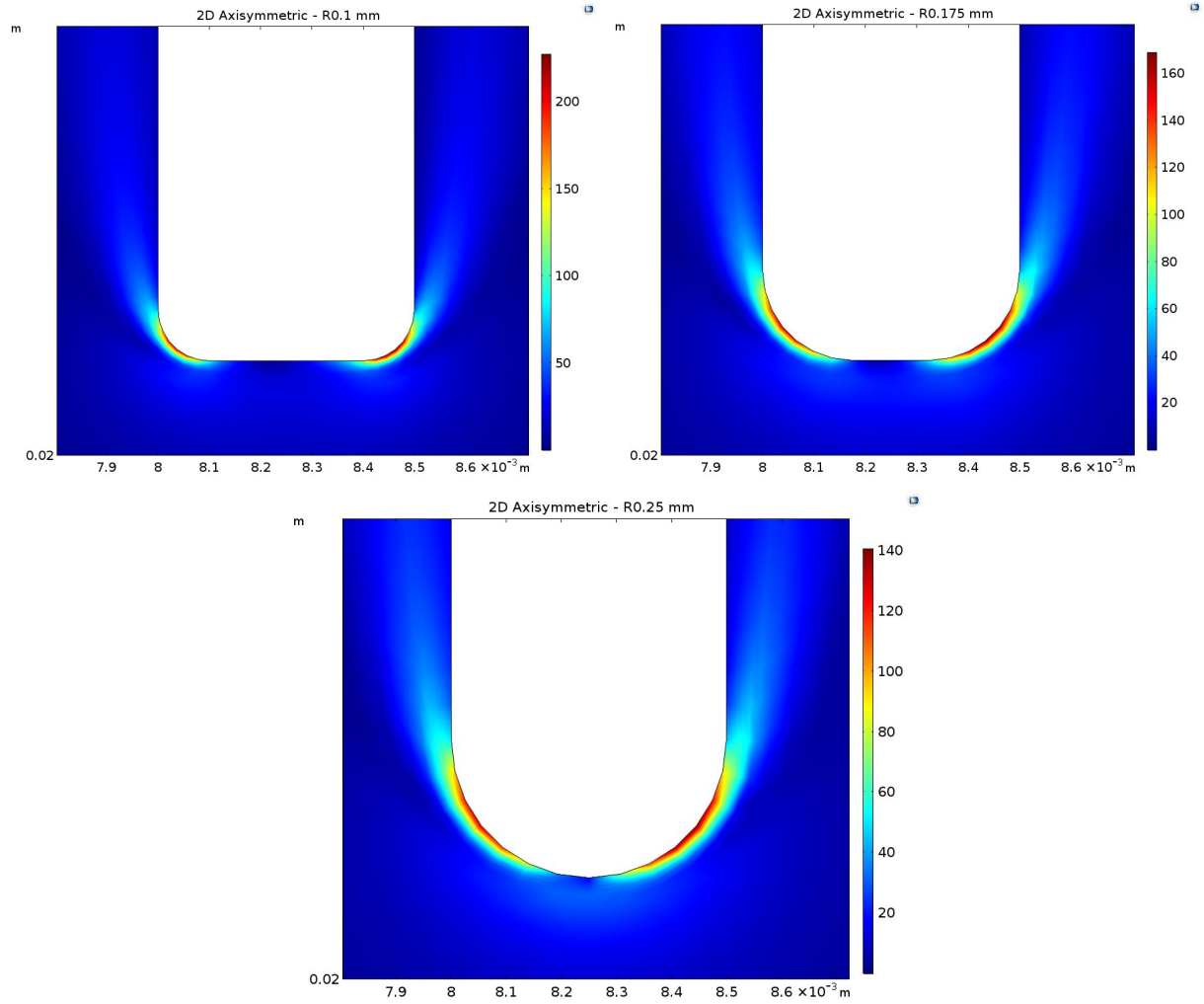

Figure 24: Leading edge shear stresses on a 2D Axisymmetric Model.

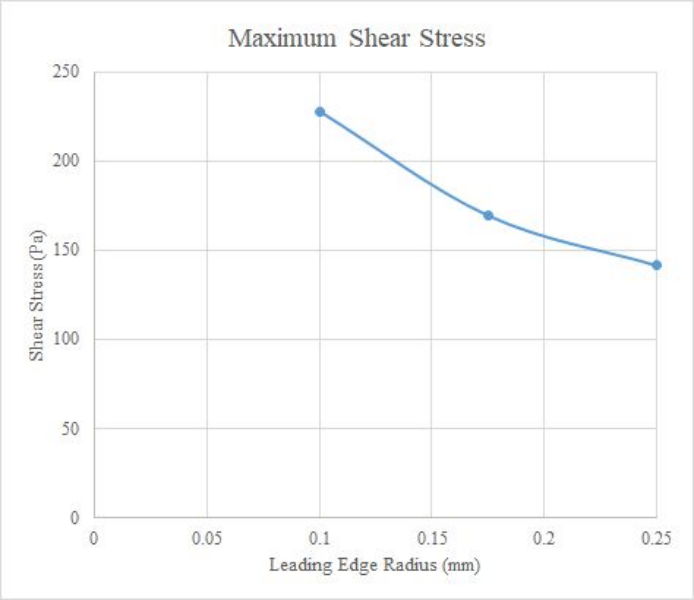

Figure 25: The shear stress is minimized by a larger leading edge radius

Additionally, it is interesting to note that since increasing the leading edge radius decreases shear stresses in the area, it is likely that thickening the leaflets could reduce shear stress, if the thicker leaflets were paired with accompanying larger leading edge radii. Thickening the leaflets results in a variety of other effects to valve performance, but by utilizing a computer model, one could run optimization analyses to find the ideal leaflet thickness that results in the best combination of performance attributes (e.g. leading edge shear stress, valve closing/opening dynamics, etc).

12.2 Leaflet Curvature

The second design input one could glean from our analysis is in regards to the importance of the leaflet curvature. Shear stresses and resultant platelet damage are elevated over the entire leaflet surface, to a magnitude greater than that seen on bileaflet valve surfaces. This indicates that the particular geometry of the leaflet causes higher shear stresses, likely due to the thin flow regions that the trileaflet valve creates between the leaflets and the annulus. Optimizing the curvature of the leaflets would likely reduce platelet damage from this effect.

13.0 Future Improvements to Model

Moving forward there are a number of improvements that could be made to model to improve the accuracy of analyzing the effects of platelet thrombogenicity. The first main aspect of the model that could be incorporated is the modelling of the aortic arch. This would improve the accuracy of parameter measurements downstream as the velocity profile will be forced to skew toward the artery wall along the inside of the arch. This improvement will have introduce computing restraints as it was seen that modelling a full model with only a linear region experienced computing times beyond 24 hours.

The next improvement to the model that could be implemented the incorporation of a dynamic simulation with fluid-structure interaction. Allowing for a time dependent study to analyze the entire cardiac cycle

would be beneficial to also observe where shear stress may also be high in relation to the valve leaflet. This would also be beneficial in observing affects in the closing period of the valve and comparing the effects of platelet damage which could ultimately provide insight into design considerations for the valve leaflet. While this may be an ideal improvement to the model, incorporating a time dependent study will also introduce computational limits.

Lastly the final improvement that could be offered to the model is the inclusion of the hinge mechanisms to the heart valve. This would be an important feature to add based upon the results showing that peak shear stresses were present along the leaflet surface. Similarly the velocity was high around and behind the leaflet due to recirculation. Therefore incorporating these aspects of the valve could provide insight to how different hinge designs may affect platelet damage as well velocity profiles around the leaflet. Offering this improvement may introduce a number of geometric and mesh complications.

14.0 Appendix

Because of the conflicting literature, we sought to validate our symmetry assumption by running a coarse mesh full model and comparing it to 1/3rd and 1/6th model of equivalent mesh density. For all models, the following mesh restrictions were implemented:

Table 4: Mesh size for comparison of full and 1/6th model

	Maximum Element Size (mm)	Minimum Element Size (mm)
Walls	1.66	0.494
Leaflet Faces	1.31	0.247
Leaflet Edges	1.31	0.247

There exist many discrepancies between the three models, as shown in the figure and table below.

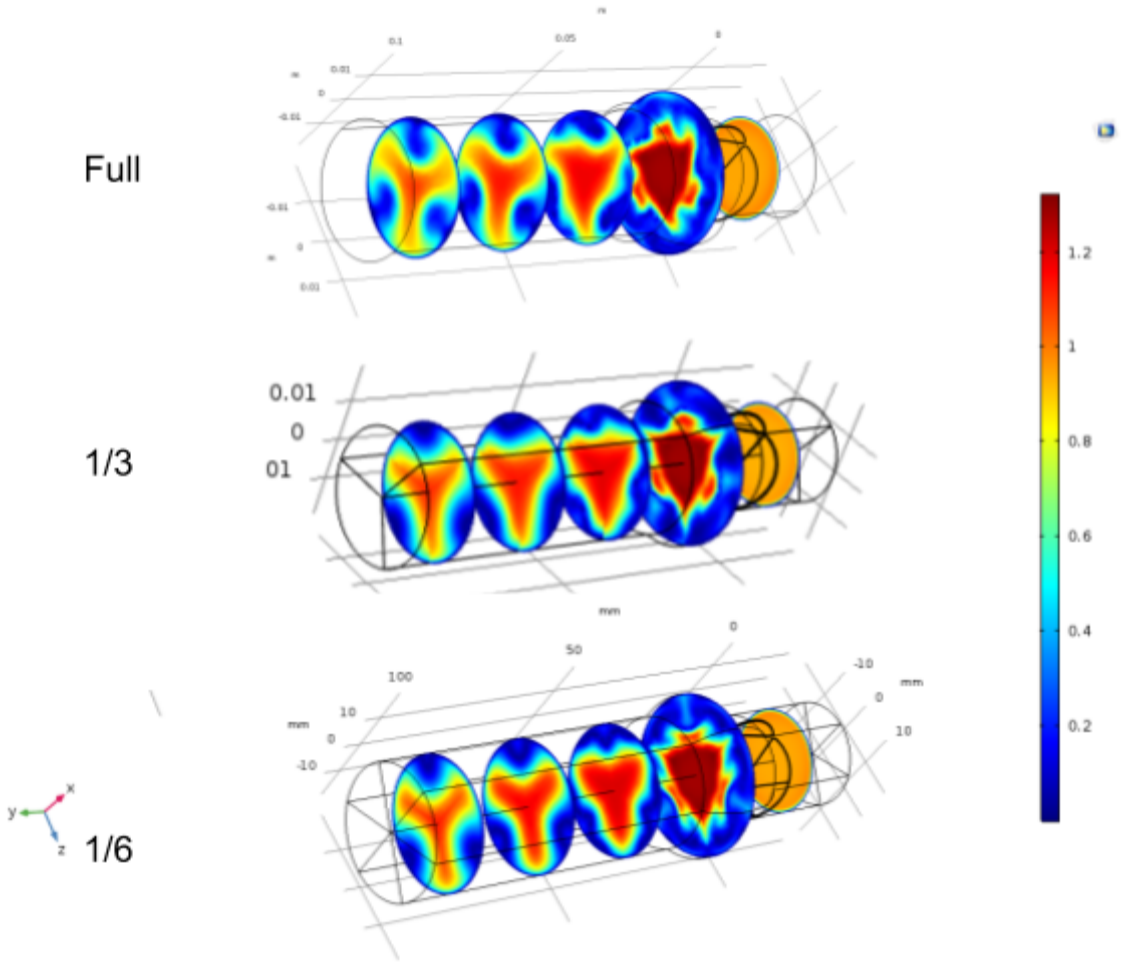

a.

b.

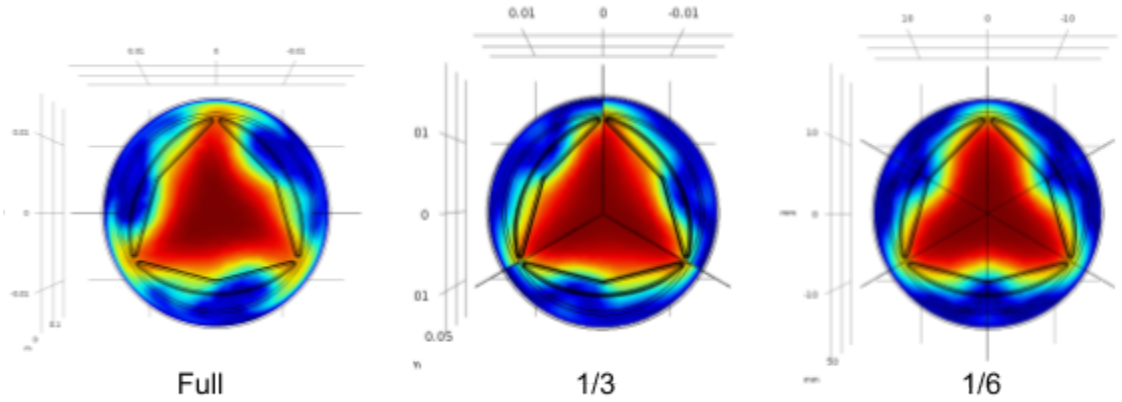

Figure 26: (a) Slice plot of full, ⅓ and ⅙ symmetry model. (b) Cross section of velocity profile of full, ⅓, and ⅙ models.

Table 5: Comparison of maximum values of velocity and shear stress in the full and 1/6th symmetry models.

	Maximum Velocity (m/s)	Maximum Shear Stress (Pa)
Full Model	1.5539	236.64
1/3rd Model	1.5488	217.88
1/6th Model	1.5789	254.53

There are several possible explanations for the differences between the three models. One important consideration is the coarse mesh used for comparison. While finer meshes were run for both the 1/6th and 1/3rd models, it was not possible to run the full model at a finer mesh due to computation time. However, there were noticeable differences in the solutions at different mesh densities for the symmetry models, indicating that the above depiction of the full model is not necessarily reflective of the true solution.

While we acknowledge that the best course of action would be to proceed with the full model, the long computational time makes this unfeasible. The 1/3rd model was therefore utilized as this is the model most consistent with the literature and seems to show the asymmetry across the valve demonstrated by the full model.

14.1 Particle Tracking Convergence

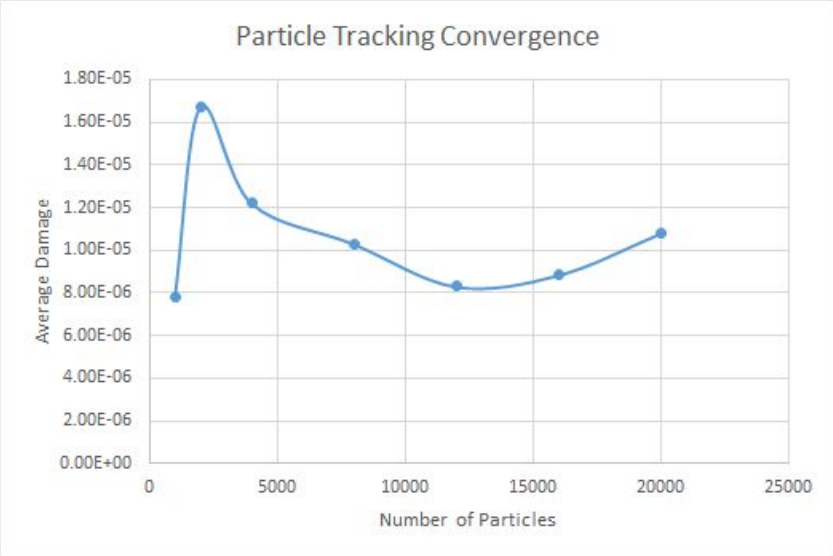

Figure 27: The average damage on the particles appears to vary somewhat randomly as the number of particles increases.

References

Alemu, Y., & Bluestein, D. (2007). Flow-induced Platelet Activation and Damage Accumulation in a Mechanical Heart Valve: Numerical Studies. Artificial Organs, 31(9), 677-688. doi:10.1111/j.1525-1594.2007.00446.x

Celik, T., Balta, S., Ozturk, C., & Iyisoy, A. (2016). Whole Blood Viscosity and Cardiovascular Diseases: A Forgotten Old Player of the Game. Medical principles and practice : International journal of the Kuwait University, Health Science Centre, 25(5), 499–500. doi:10.1159/000446916

Dasi, L. P., Helene, S. A., Sucosky, P., & Yoganathan, A. P. (n.d.). Fluid Mechanics of Artificial Heart Valves. Clinical and Experimental Pharmacology and Physiology, 36(2), 225-237.

Garcia, Julio et al. "Distribution of blood flow velocity in the normal aorta: Effect of age and gender." Journal of magnetic resonance imaging : JMRI vol. 47,2 (2017): 487-498. doi:10.1002/jmri.25773, https://www.ncbi.nlm.nih.gov/pmc/articles/PMC5702593/

Heart Valve Repair or Replacement. (n.d.). Retrieved February 20, 2019, from https://www.texasheart.org/heart-health/heart-information-center/topics/valve-repair-or-replacement/

Hellums JD, Peterson DM, Stathopoulos NA, Moake J. Studies on the Mechanisms of Shear-Induced Platelet Activation. In: Hartmann A, Kuschinsky W, editors. Cerebral Ischemia and Hemorheology.Heidelberg: Springer-Verlag; 1987. pp. 80–89 https://www.ncbi.nlm.nih.gov/pmc/articles/PMC3640664/

Hojin, Ha et al. Age-Related Vascular Changes Affect Turbulence in Aortic Blood Flow , Frontiers in Physiology vol. 9 (2018): https://www.frontiersin.org/articles/10.3389/fphys.2018.00036/full

Kadhim, S. K., Nasif, M. S., Al-Kayiem, H. H., & Al-Waked, R. (2017). Computational fluid dynamics simulation of blood flow profile and shear stresses in bileaflet mechanical heart valve by using monolithic approach. Simulation, 94(2), 93-104. doi:10.1177/0037549717712603

Li, C., & Lu, P. (2012). Numerical comparison of the closing dynamics of a new trileaflet and a bileaflet mechanical aortic heart valve. Journal of Artificial Organs, 15(4), 364-374. doi:10.1007/s10047-012-0650-8

Nobili, Matteo et al. "Platelet activation due to hemodynamic shear stresses: damage accumulation model and comparison to in vitro measurements." ASAIO journal (American Society for Artificial Internal Organs : 1992) vol. 54,1 (2008): 64-72. doi:10.1097/MAT.0b013e31815d6898, https://www.ncbi.nlm.nih.gov/pmc/articles/PMC2756061/

Sheriff, Jawaad et al. “Evaluation of shear-induced platelet activation models under constant and dynamic shear stress loading conditions relevant to devices.” Annals of biomedical engineering vol. 41,6 (2013): 1279-96. doi:10.1007/s10439-013-0758-x https://www.ncbi.nlm.nih.gov/pmc/articles/PMC3640664/#R8

Stevenson, Dana M et al. Numerical Simulation of Steady Turbulent Flow Through Trileaflet Aortic Heart Valves II. Results on Five Models, J. Biomechanics Vol. 18, No. 12, pp. 909-926 (1985).

Woo, Yi-Ren et al, In Vitro Pulsatile Flow Velocity And Shear Stress Measurements In The Vicinity Of Mechanical Mitral Heart Valve Prostheses, Journal of Biomechanics vol 19, No. 1. Pp 39-51 (1986)

Woo, Yi-Ren et al, (1986), Pulsatile flow velocity and shear stress measurements on the st. jude bileaflet valve prosthesis, Scandinavian Journal of Thoracic and Cardiovascular Surgery, 20:1, 15-28, DOI: 10.3109/14017438609105910